Academic Journal of Science and Technology
ISSN: 2771-3032 | Vol. 7, No. 2, 2023

Research on Active Disturbance Rejection Control of Brushless DC Motor Based on Vector Control

Yuxin Wang

School of Electrical Engineering, Southwest Minzu University, Chengdu, Sichuan 610041, China

Abstract: A Active Disturbance Rejection Control strategy based on vector control is proposed to address the problems of poor speed overshooting immunity in the control system of brushless DC motor. The motor magnetic chain and torque are decoupled by vector control method to simplify the control, and the traditional PI controller in the speed loop is replaced by a active disturbance rejection controller. The transition process is arranged by tracking differential (TD) to smooth the given speed, which overcomes the contradiction between speed overshoot and rapidity, and improves the response capability of the system; a second-order extended state observer (ESO) is introduced, which estimates and compensates the total system disturbance and improves the system's immunity to disturbance; and the nonlinear law state error feedback (NLSEF) is utilized by the Through the nonlinear law state error feedback (NLSEF), the control accuracy of the system is improved by utilizing the nonlinear control principle of "large gain with small error and small gain with large error". The simulation results show that the control strategy proposed in this paper is characterized by fast response, no overshooting, strong resistance to load disturbance, and strong robustness to changes in load and speed, which proves the feasibility and advancement of this strategy.

Keywords: Brushless dc motor, Active disturbance rejection control, Vector control, Speed-current double closed loop.

1. Introduction

As a big country of rare earth resources, with the current continuous development of power electronics technology, computer control technology, materials science and other fields, brushless DC motors (BLDCM), which are made of permanent magnet materials, are being more and more widely used in industrial manufacturing and daily life. However, BLDCM is a complex system with many internal variables and obvious nonlinear characteristics, which makes it difficult to establish a high-precision dynamic mathematical model for it. [1] It is difficult to establish a high-precision dynamic mathematical model for it. Therefore, in order to meet the demand for more accurate control, more advanced motor control strategies are needed. The traditional PID control algorithm has become one of the most commonly used control algorithms in the field of motor control due to its simple structure and ease of application in engineering practice. [2] However, the traditional PID control algorithm has been used as one of the most common control algorithms in motor control. However, the traditional PID control algorithm is mainly based on linear model, strong dependence on parameters, and poor anti-interference ability, and can not meet the high precision requirements of the control system. [3] The traditional PID control algorithm is mainly based on linear model, which has strong dependence on parameters and poor anti-interference ability, and cannot meet the high precision requirements of control system. Therefore, the research of a higher performance brushless DC motor control system has become the research direction of many scholars around the world. Because the brushless DC motor control system is a multivariable coupling system in the three-phase natural coordinate system, it is difficult to control the complex relationship between the magnetic chain and the torque of the motor. [4] The vector control technology can combine the magnetic chain and torque with the magnetic chain and the torque. Vector control technology can decouple the complex relationship between magnetic chain and torque, which not only makes the system have faster response speed, but also makes the control process simple to a certain extent. [5] Therefore, this paper applies it to the control of brushless DC motor system.

With the research carried out in recent years, adaptive control [6] and fuzzy control [7] and neural network control [8] and other theories have been fully developed. However, although these methods have achieved better control effects in theory, they are difficult to be applied in practice due to the complexity of their realization.

Active Disturbance Rejection Control (ADRC) is a new type of nonlinear control theory that does not depend on the exact mathematical model of the object, proposed by Kyung-Ching Han [9] ADRC is a new nonlinear control theory that does not depend on the exact mathematical model of the object. Many results have been achieved in the application as well as improvement of the active disturbance rejection controller. Among them, the literature [10] model-compensated self-oscillatory controller is used to replace the traditional self-oscillatory controller, but it is easy to lead to the saturation of the control volume and does not achieve the optimal compensation effect. Literature [11] A method of speed-loop smooth-mode active disturbance rejection control based on internal-mode observation is proposed to improve the problem of poor speed regulation performance due to motor load disturbance. Literature [12] A feed-forward compensation based active disturbance rejection control algorithm is used to control a brushless DC motor and applied to an electric valve, resulting in a significant improvement in position control accuracy and immunity. Literature. [13] A fuzzy control strategy combining fuzzy control and self-resistant control is proposed to control the yarn constant tension of a brushless DC motor, which makes the fluctuation range of the yarn tension smaller and the response of the system faster. Literature [14] A parameter active disturbance rejection control method based on the improved particle swarm algorithm is designed and applied to the linear active disturbance rejection controller, which greatly simplifies the

steps of parameter tuning.

In this paper, for the problems of poor anti-interference ability, speed overshooting and large torque fluctuation of the brushless DC motor under the control of traditional PID algorithm, a control strategy based on active disturbance rejection control is proposed to apply the active disturbance rejection controller to the speed loop of the brushless DC motor control system. On the basis of establishing a mathematical model of the brushless DC motor, the general derivation process of the speed loop active disturbance rejection controller is given. The performance of the brushless DC motor control system under the active disturbance rejection controller is investigated by modeling simulation in Simulink. The simulation results show that the system performance under this control strategy is excellent, with fast response, no overshoot, etc., and can effectively resist load perturbations and is robust to load variations and speed variations. This further confirms the effectiveness and feasibility of the strategy.

2. Mathematical Model of Brushless DC Motor

The mathematical model of the motor can be represented as follows in the d-q synchronous rotating coordinate system:

The motor stator voltage equation is:

$$\begin{cases} u_d = R_s i_d + L_d \dfrac{di_d}{dt} - \omega_e \psi_q \\ u_q = R_s i_q + L_q \dfrac{di_q}{dt} + \omega_e \psi_d \end{cases} \tag{1}$$

Where: u_d , u_q are d, q-axis voltage; i_d , i_q are d, q-axis current; ψ_d , ψ_q are d, q-axis magnetic chain; L_d , L_q are d, q-axis inductance; ω_e is the motor rotor electric angular velocity.

The motor stator magnetic chain equation is:

$$\begin{cases} \psi_d = L_d i_d + \psi_f \\ \psi_q = L_q i_q \end{cases} \tag{2}$$

Where: ψ_f is the magnetic chain of the permanent magnet.

The motor torque equation is:

$$\begin{aligned} T_e &= 1.5 P_n (\psi_d i_q - \psi_q i_d) = \\ & 1.5 P_n \left[\psi_f i_q + (L_d - L_q) i_d i_q \right] \end{aligned} \tag{3}$$

Where: T_e is the electromagnetic torque; P_n is the number of motor pole pairs.

Taking the brushless DC motor with surface-mounted rotor structure as the object of study, there is $L_d = L_q$, and the control strategy of $i_d = 0$ is used, at this time, Eq. (3) can be rewritten approximately as:

$$T_e = 1.5 P_n \psi_f i_q \tag{4}$$

The motor equation of motion is:

$$T_e - T_L = J \frac{d\omega_m}{dt} + B\omega_m \tag{5}$$

Where: T_L is the load torque; J is the rotational inertia; B is the viscous coefficient; ω_m is the mechanical angular velocity.

3. Active Disturbance Rejection Controller Design

3.1. Introduction to active disturbance rejection control

As a kind of nonlinear control algorithm, the core idea of ADRC is to avoid overshooting by arranging the transition through the tracking differentiator (TD), to compensate the total disturbances inside and outside the system as the state quantities for the observation and estimation by the expansion observer (ESO), and to obtain the final output quantity through the nonlinear feedback law of nonlinear error (NLSEF) by nonlinearly feeding back the errors of the first two phases. The structure is shown in Fig. 1.

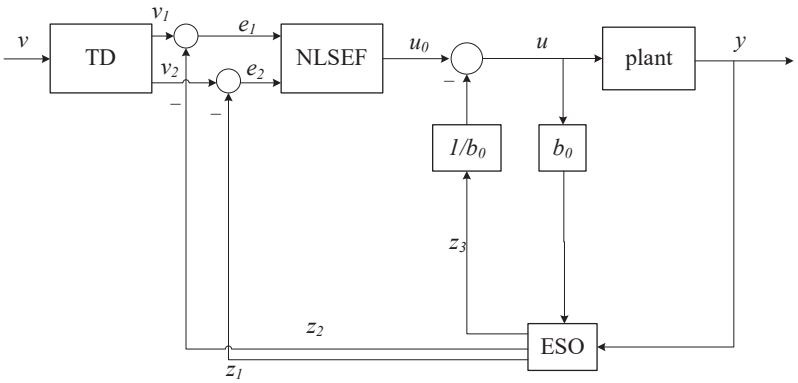

Figure 1. Block diagram of ADRC structure

The TD module helps in smoothing the transition of the input signal v where v_1 is used for fast tracking of the input signal and v_2 is the differential signal of the input signal. the ESO module is capable of observing the state variables of the system where z_1 is the tracking signal of the output y, z_2 is the approximate differential of the output y *and* z_3 is used for observing the total system perturbation. The error signals e_1 and e_2 , which are one of the input signals to the NLSEF module, are obtained by differencing v_1 , v_2 and z_1 , z_2 respectively. After the NLSEF has processed the input error signals, the output signal u_0 is output and the system is converted to an integrator series system.

for a typical first-order system:

$$\dot{y} = f(y, \omega(t), t) + bu \tag{6}$$

where $\omega(t)$ is the value of external disturbance; f is the value of total disturbance; u is the control quantity of the system. At this point, by making $y=x$, the state equation of the system can be obtained:

$$\begin{cases} \dot{x} = f(x, \omega(t), t) + bu \\ y = x \end{cases} \tag{7}$$

The core of ADRC is to utilize the ESO module to observe and estimate the total disturbance of the system, while compensating for it by using the error feedback control law module to turn the system into a standard integrator series type system for simplified control.

3.2. Speed loop ADRC design

3.2.1. Velocity loop TD design

Arranging the transition process for the input speed signal of the BLDC control system, the following mathematical model is obtained [15] :

$$\begin{cases} e_1 = z_{11} - y^* \\ \dot{z}_{11} = -rfal(e_1, \alpha_1, \delta_1) \end{cases} \tag{8}$$

The fal function in Eq. (11) is defined as follows:

$$fal(e, \alpha, \delta) = \begin{cases} |e|^{\alpha} sign(e) & |e| > \delta \\ \dfrac{e}{\delta^{1-\alpha}} & |e| \le \delta \end{cases} \tag{9}$$

In this equation, the variable r represents the speed of the control tracking signal, which is proportional to the tracking speed. z_{11} is the speed signal after smoothing transition, y^* is the given speed signal, and δ_1 is the filtering factor, α is usually taken as 0.5 or 0.25.

3.2.2. Velocity loop ESO design

Mathematical modeling of ESO for BLDC velocity loops [16] for:

$$\begin{cases} e_2 = z_{21} - y \\ \dot{z}_{21} = z_{22} - \beta_{21} fal(e_2, \alpha_2, \delta_2) + bu \\ \dot{z}_{22} = -\beta_{22} fal(e_2, \alpha_3, \delta_2) \end{cases} \tag{10}$$

In this equation, z_{21} represents the observed value of the actual output y, z_{22} is an estimate of the total system perturbation, and the filtering factor δ_3 . The parameters to be adjusted are β_{21} and β_{22} , and e_2 is *t*he value of the error between the observed value z_{21} and the actual output signal y. The filtering factor δ *i*s a parameter of β and β .

3.2.3. Velocity loop NLSEF design

The NLSEF mathematical model of BLDC speed loop is designed as follows:

$$\begin{cases} e_3 = z_{11} - z_{21} \\ u_0 = \beta_{33} fal(e_3, \alpha_4, \delta_3) \\ u = u_0 - \dfrac{z_{22}}{b} \end{cases} \tag{11}$$

In this equation, e_3 represents the error between the velocity signal z_{11} after arranging the transition process and the observed value z_{21} of the actual output y, while $-z_{22}/b$ denotes the component of the compensating perturbation.

From Eqs. (3) and (5), we have that under the control strategy of i_d =0:

$$\begin{aligned} \frac{d\omega_m}{dt} &= \frac{1.5 P_n \psi_f i_q - T_L - B\omega_m}{J} \\ &= \frac{1}{J} 1.5 P_n i_q \psi_f - \frac{1}{J}(B\omega_m + T_L) \end{aligned} \tag{12}$$

From the equation (12) it can be seen that i_q , T_L , ω_e and other factors have influence on the motor speed. Taking i_q as the variable to be controlled, the other factors can be regarded as the total perturbation, then the total perturbation is:

$$a(t) = -\frac{1}{J}(B\omega_m + T_L) \tag{13}$$

Then equation (6) can be rewritten as:

$$\frac{d\omega_m}{dt} = \frac{1}{J} 1.5 P_n \psi_f i_q + a(t) \tag{14}$$

According to Section 2.1, the current i_q is used as the control quantity and the given signal ω_m * and the actual rotational speed are used as inputs to the ADRC controller, then the BLDCM speed loop can be regarded as a first-order system.

4. Simulation Study and Result Analysis

This chapter will compare the performance of the speed loop of the brushless DC motor control system under the self-immobilizing controller and the PI controller, including motor performance indexes such as rated speed response, load-disturbed speed response, and response robustness under different speed settings. The effectiveness and feasibility of the self-immobilizing controller for improving the performance of the brushless DC motor control system will be verified through comparative analysis.

4.1. Simulink model construction

The model is built by MATLAB/Simulink to verify the validity and reliability of the self-immunity controller. The basic block diagram is shown in Fig. 2 and Fig. 3

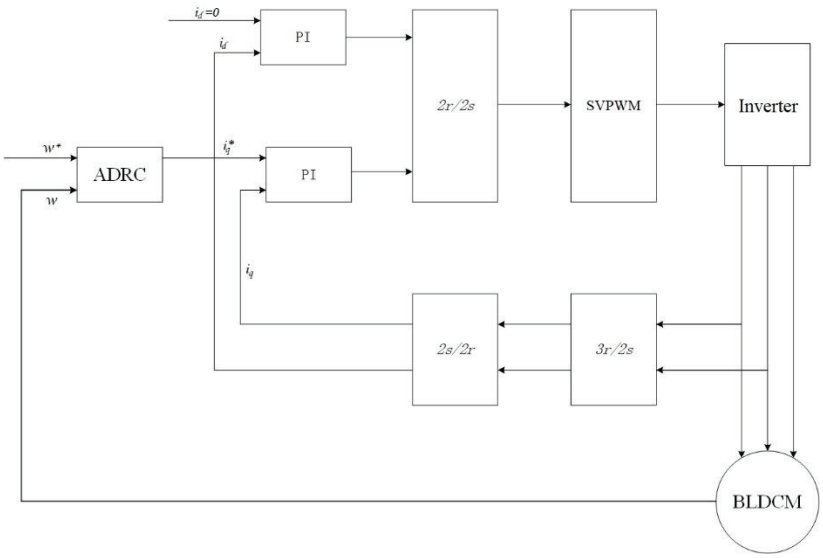

Figure 2. Block diagram of brushless DC motor control system based on self-immunity control

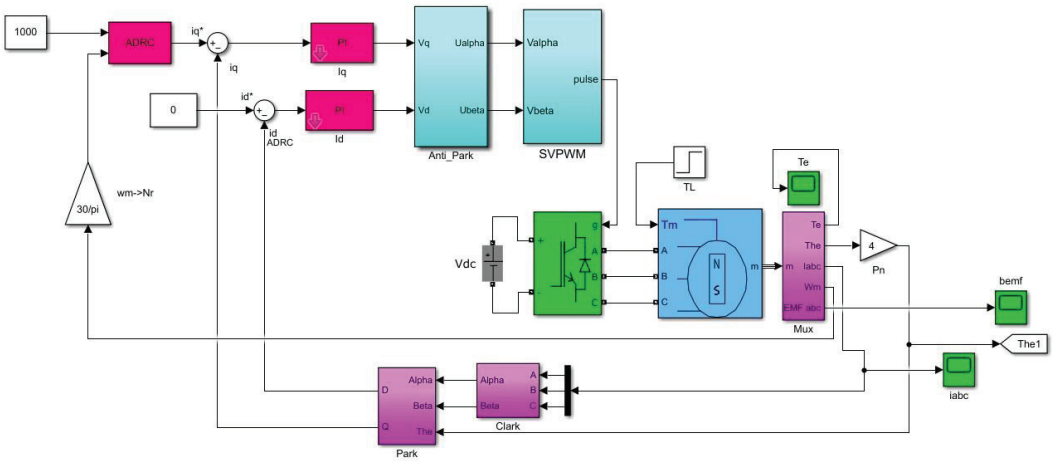

Figure 3. Simulation diagram of self-immunity controller

The parameters of the brushless DC motor in the simulation are as follows: the number of pole pairs P_n = 4; stator inductance L_s = 8.5 mH, stator resistance R_s = 0.96 Ω, permanent magnet chain ψ_f = 0.183 Wb, rotational moment of inertia J = 0.003 kg- m^2 , hysteresis coefficient B = 0.008 N-m^2 , rated speed of 1000 r/min, and rated voltage of 311V.

4.2. Simulation results and analysis

4.2.1. Rated speed response

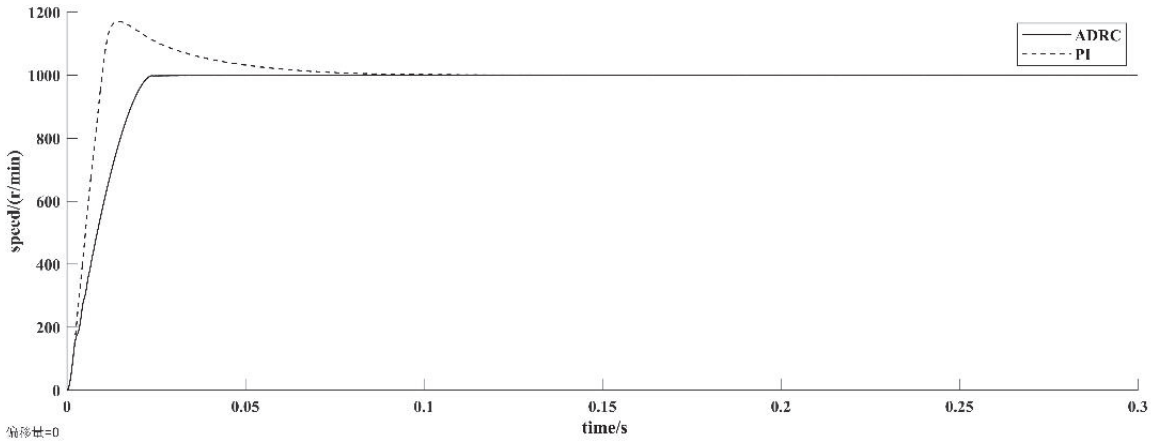

Figure 4. Motor speed response waveform at rated speed

A comparison of the simulated waveforms of ADRC and PI control at rated speed is shown in Fig. 4. At a given rated speed of 1000 r/min, the ADRC-controlled motor reaches the specified speed in about 0.025 s with no overshoot.

While the motor controlled by the traditional PI controller has a significant overshoot of 17% although the start-up

response is slightly higher than that of the motor controlled by the ADRC, this is because the ADRC has set up a tracking differentiator (TD) to arrange the transition process in order to balance the contradiction between the rapidity of the system's start-up response and the overshoot.

4.2.2. Resistance to load torque disturbances

Without changing any parameter, a 5N-m load is added at 0.2s, as shown in Fig. 5, the amplitude of speed fluctuation and the time taken to recover to the rated speed of the motor controlled by the PI controller are much larger than that of the motor controlled by ADRC, indicating that the ADRC algorithm has better anti-interference ability under loaded conditions.

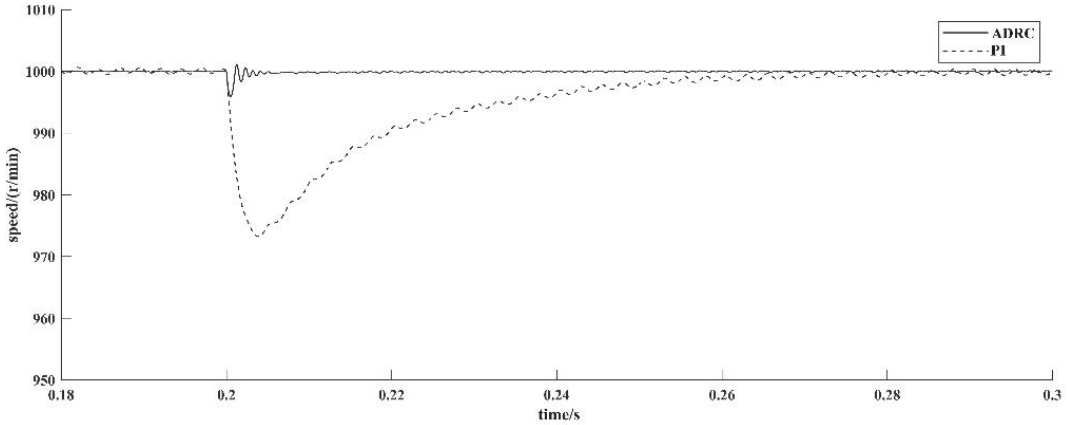

Figure 5. 0.2s sudden load motor speed response curve

4.2.3. Speed Response at Different Speed Settings

In order to continue to verify the performance of the ADRC strategy, under the condition of keeping the system parameters unchanged, the rotational speed was set to 0.8 times and 1.2 times the rated speed, as well as the forward and reverse rotation, acceleration and deceleration experiments were carried out at the rated speed, respectively, and the resultant waveform graphs are shown in Figs. 6 to 9.

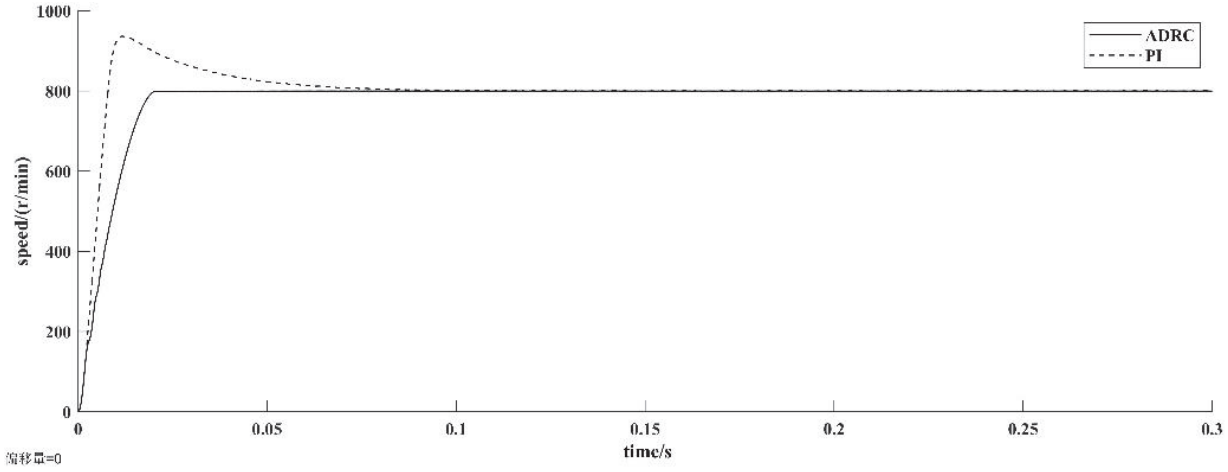

Figure 6. Motor speed response for set value 800r/min

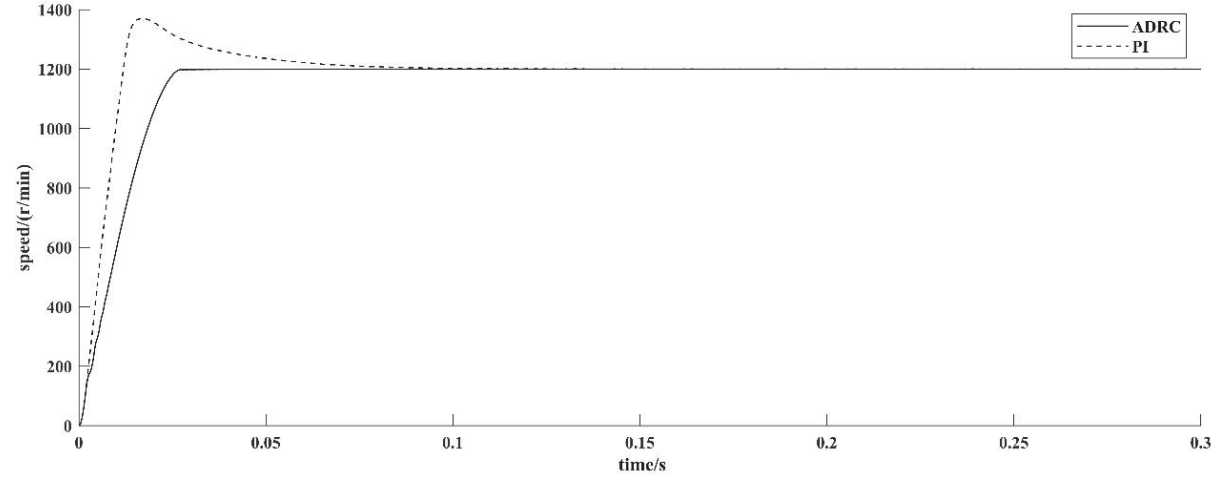

Figure 7. Motor speed response for set value 1200r/min

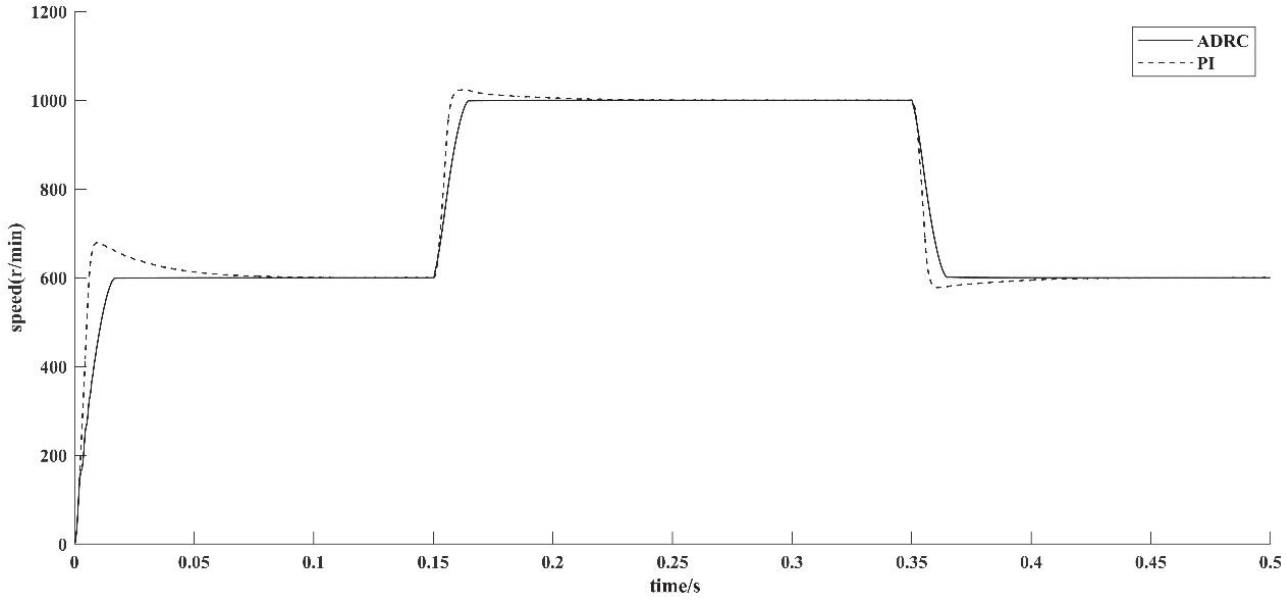

Figure 8. Motor acceleration and deceleration speed response

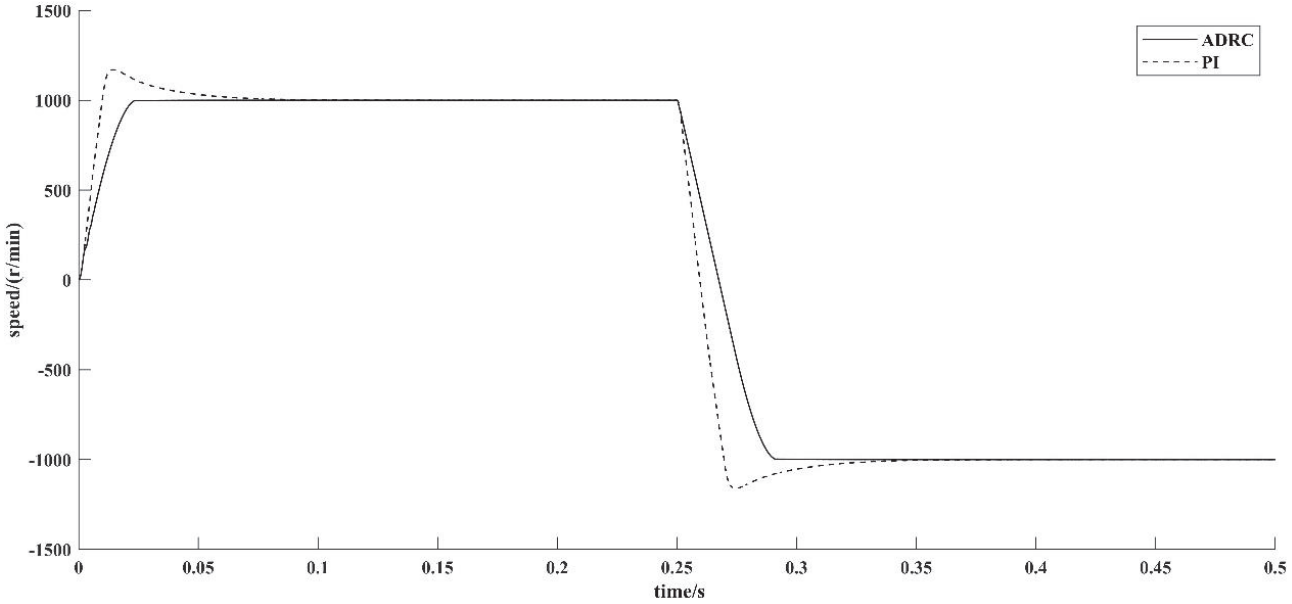

Figure 9. Forward and reverse speed response at rated speed

The above experimental results surface that when the rotational speed is 0.8 and 1.2 times of the rated speed, the rotational speed waveform response results in a better control effect compared to the traditional PI control. In the case of the initial speed set to 600r/min, the speed is increased to the rated speed of 1000r/min in 0.15s, and then reduced to 600r/min in 0.35s, the experimental results show that the system is fast and free of overshooting, and has a better control performance compared with the traditional PI control. At 0.25s, the speed is set to -1000r/min, and the motor under ADRC control is still free of overshooting and has good rapidity.

4.2.4. Comparison of other indexes under rated speed with load

The simulated waveforms of d-axis current, torque, and three-phase current of a brushless DC motor at rated speed with load are investigated to gain a deeper understanding of the control performance of the two controllers through comparison.

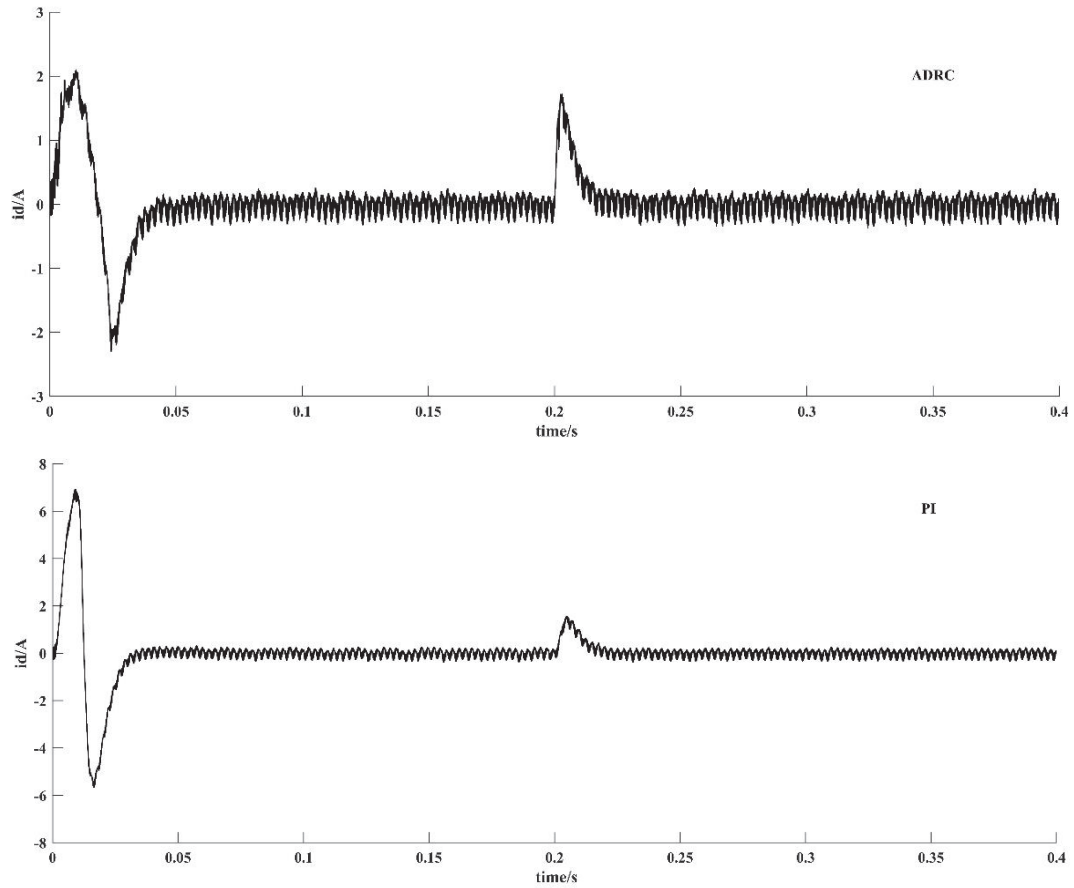

Figure 10. Comparison of motor d-axis current waveforms at rated speed with load

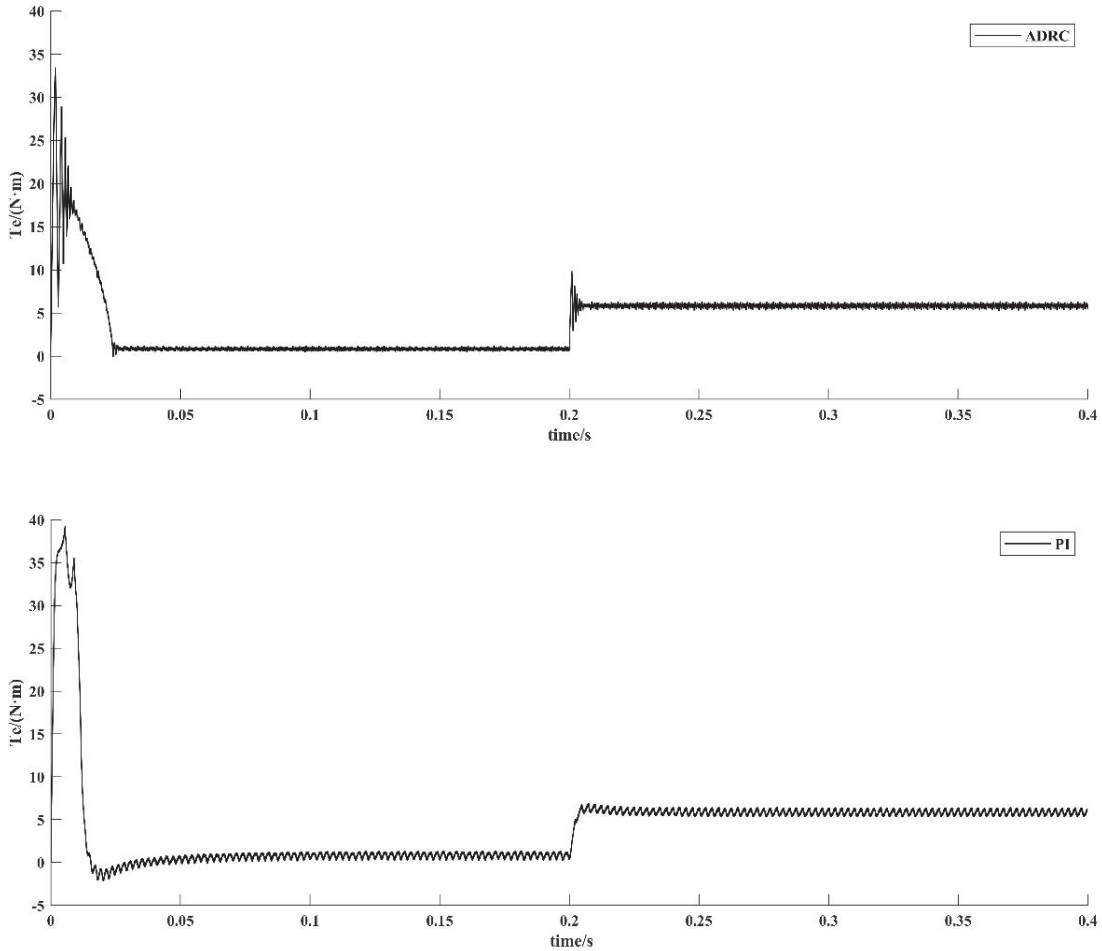

Figure 11. Comparison of electromagnetic torque waveforms of motors at rated speed with loads

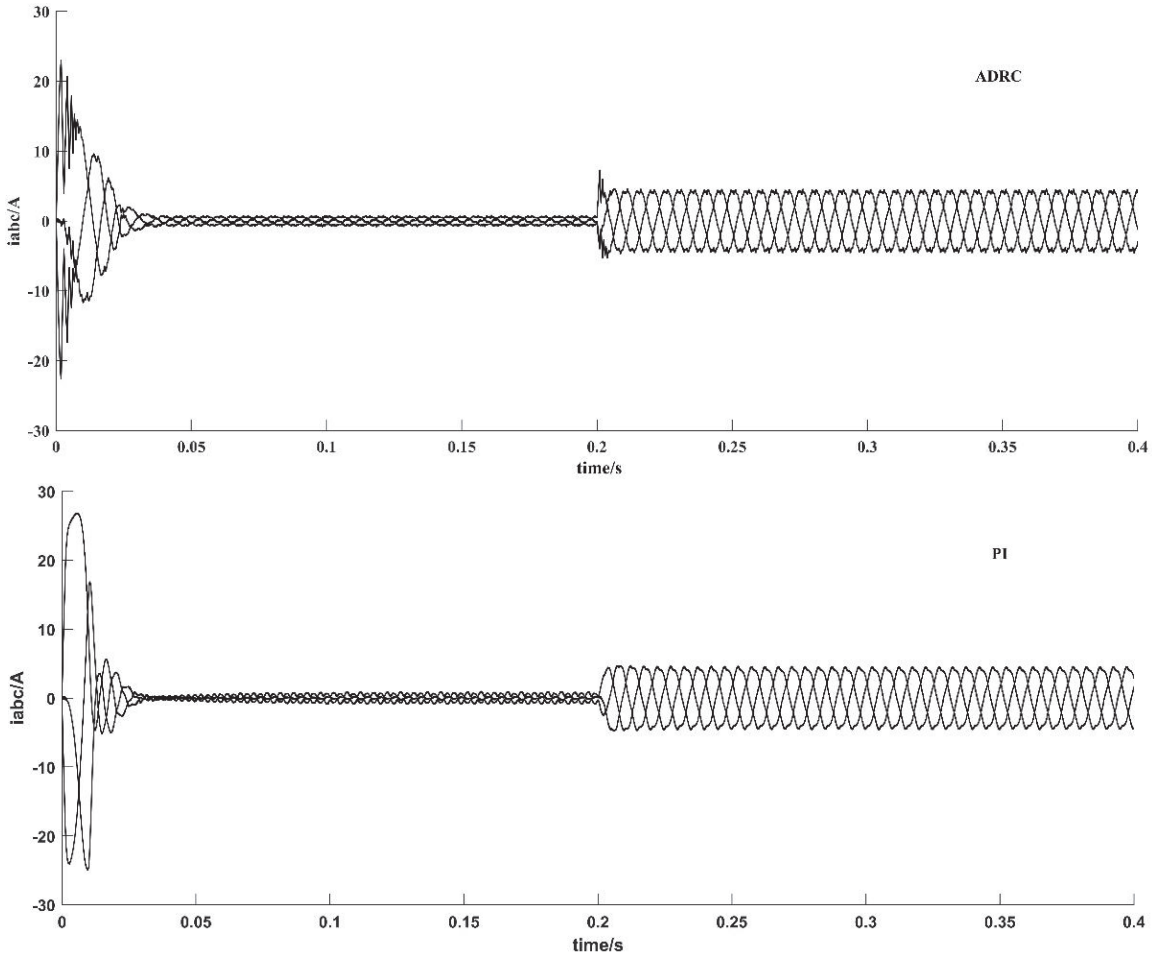

Figure 12. Comparison of three-phase current waveforms of motor at rated speed with load

Fig. 10 shows the comparison of the d-axis current waveforms at the rated speed of the motor with load, through which it can be seen that the d-axis current under the ADRC strategy is active in the range of about [-2.3,2.1], and the d-axis current under the PI strategy is active in the range of about [-5.8,6.9]. The above results indicate that the performance of the d-axis current loop of the brushless DC motor under the ADRC strategy performs better as compared to the PI strategy.

Fig. 11 shows the comparison of the electromagnetic torque waveforms under the rated speed of the motor with load, and it can be seen by comparison that the starting maximum electromagnetic torque of the motor under the ADRC strategy is about 33 N-m, and the starting maximum torque of the motor under the PI strategy is about 39 N-m, and the starting maximum torque of the motor under the control of the ADRC strategy is smaller, and the torque waveforms are smoother as a whole, which shows a better starting performance.

Fig. 12 shows the comparison of the three-phase current waveforms of the motor at rated speed with load. It can be seen from the comparison that the three-phase current peaks of the motor under the ADRC strategy are smaller as compared to that of the PI strategy, and it also shows a better control performance.

Based on the comparison of the above simulation waveforms, the vector control-based active disturbance rejection control strategy for brushless DC motor proposed in this paper is feasible and effective, balancing the contradiction between starting rapidity and overshooting, and improving the system's immunity to interference, while possessing stronger robustness.

5. Conclusion

The research objective of this paper is to address the problems of large speed response overshoot and poor interference immunity in the traditional PI-controlled brushless DC motor system, and to propose a vector control-based active disturbance rejection control strategy, which utilizes vector control to decouple the complex relationship between the magnetic chain and torque to simplify the control, and then introduces the active disturbance rejection controller into the motor speed ring, gives the general design method of the speed ring active disturbance rejection controller, and Comparison is made with the traditional PI control strategy. The results show that the control strategy proposed in this paper solves the problem of speed overshooting, and has better anti-interference ability and improves the robustness of the system, which proves the effectiveness and advancement of the system. However, this strategy still has room to improve the response performance of the system under disturbances such as sudden load change, and the anti-disturbance ability needs to be strengthened.

References

[1] Pan Xiaolei, Zhao Chuan, Lv Haili. Research on fuzzy adaptive P1D control of brushless DC motor[J] Electromechanical T program technology, 2016(3):85-89.

[2] WANG Yang,DING Zhigang,ZHENG Shuquan,et al. Design and implementation of a user profiling system[J]. Computer Application and Software,2018,35(3):8-14.

[3] CHEN D,ZHANG Q,CHEN G,et al. Forum user profiling by incorporating user behavior and social network connections [C]/ /International conference on cognitive computing. seattle:springer,2018:30-42.

[4] Han, Song-Suan. Research on position sensor-less control strategy of permanent magnet synchronous motor with full speed range[D]. Beijing:Beijing Jiaotong University Master Dissertation,2018: 41-42.

[5] ZHANG Zhuang. Research and implementation of permanent magnet synchronous motor speed control system [D]. Chengdu:Master's thesis of University of Electronic Science and Technology,2018: 15-17

[6] SONG Lijun,WANG Yan. A fuzzy adaptive control method for brushless DC motor[J]. Manufacturing Technology and Machine Tools, 2022(4):145-148. DOI:10.19287/j.mtmt.1005-2402.2022.04.023.

[7] Liu Yuhao,Liao Ping. Fuzzy control design of brushless DC motor based on MFO algorithm[J]. Instrumentation Technology and Sensors,2021(4):107-111. DOI:10.3969/j.issn.1002-1841.2021.04.023.

[8] Liu Yuhao,Liao Ping. Fuzzy control design of brushless DC motor based on MFO algorithm[J]. Instrumentation Technology and Sensors,2021(4):107-111. DOI:10.3969/j.issn.1002-1841.2021.04.023.

[9] Han, Kyung-Ching. Expanded state observer for a class of uncertain objects[J]. Control and Decision Making,1995, (1): 85-88.

[10] ZUO Yuefei,ZHANG Jie,LIU Gang,et al. Improved active disturbance rejection controller for permanent magnet synchronous motor with time-varying input [J]. Journal of Electrotechnology, 2017,32(02):161-170.

[11] QIAO Yongming, ZHANG Chao,LIU Jinglin. Sliding mode active disturbance rejection control of brushless DC motor based on internal mode observation[J]. Micro Motor, 2023, 56(1):65-69,94.

[12] WANG Shixin,YU Bo,YU Yong,et al. Study on improved active disturbance rejection control of BLDC in electric valves[J]. Electrical Drives,2023,53(4):3-8,83.

[13] WANG Yannian, WU Yang, LU Zhifa, et al. Research on constant tension fuzzy ADRC control strategy of yarn conveyor[J]. Overseas Electronic Measurement Technology, 2021, 40(8):52-56.

[14] LI Zhen, WANG Fan, WANG Ranjun, et al. Parameter self-tuning of self-resistant controller for permanent magnet synchronous motor[J]. Computerized Measurement and Control, 2021, 29(05):92-96.

[15] Yang He. Research on the robustness improvement strategy of permanent magnet synchronous motor based on self-immunity control[D]. Harbin Institute of Technology,2021.

[16] Zheng Zheng,Zhao Laiguo. Research on PMSM positionless sensor based on adaptive sliding mode observer[J]. Journal of Wuhan University (Engineering Edition),2022,55(04):387-393+400.